Performance and Flight Characteristics of the Sandhawk Family of Rocket Systems

GERALD G. WILSON* AND WILLIAM A. MILLARD†
Sandia Corporation, Albuquerque N. Mex.

The requirement for a sounding rocket capable of carrying large and heavy payloads (79.4–385.6 kg) to high altitudes has led to the development of the 0.33-m (13-in.-diam) Sandhawk rocket motor. The Sandhawk has been flown in a single-stage configuration, as a booster for the Sandhawk-Tomahawk 9 system, and as a second stage for the Terrier-Sandhawk 13 system. A Terrier-Sandhawk 17 system is currently being developed. Expected performance, estimated payload-impact dispersion, flight characteristics, and aerodynamic data for each of these rocket systems are presented. Selected flight data are also presented.

Nomenclature

AR	= aspect ratio of fins
b	= total fin span, m
C_A	= axial force coefficient
C_{l_p}	= roll damping moment coefficient (based on $l_{ref}/2V$), rad^{-1}
C_{l_δ}	= induced rolling moment coefficient, deg^{-1}
C_{m_α}	= pitching moment coefficient slope referenced to the vehicle center of gravity, rad^{-1}
$C_{m_q} + C_{m_{\dot\alpha}}$	= pitch damping moment coefficient (based on $l_{ref}/2V$), rad^{-1}
C_{N_α}	= normal force coefficient slope, rad^{-1} or deg^{-1}
$C_{N_{\dot\alpha}}, C_{N_q}$	= normal forces due to $\dot\alpha$ and q (based on $l_{ref}/2V$), rad^{-1}
d,l	= vehicle diameter and length, m
I,I_x	= pitch and roll moments of inertia, kg $-$ m^2
M	= vehicle mass or Mach number
M_α	= pitching moment change with angle of attack, nt $-$ m/rad
M_p	= gross payload mass, kg
p,q	= roll and pitch rates, rad/sec
SM	= vehicle static margin (% l_{ref})
V	= vehicle velocity, m/sec
$X_{c.g.}, X_{c.p.}$	= vehicle center of gravity and center of pressure locations (measured from nose), m
α	= angle of attack, rad
β	= $(\lvert M^2 - 1\rvert)^{1/2}$
δ	= fin cant, rad or deg
Λ	= fin quarter chord sweep angle, rad
ξ	= d/b
ω_N	= natural pitching frequency $(-M_\alpha/I)^{1/2}$, rad/sec

Introduction

THE development of sounding or meteorological rocket systems at Sandia Laboratories was initiated in the late 1950's to support atmospheric nuclear testing. Since the inception of the nuclear test ban, the Atomic Energy Commission's test readiness programs have provided continued emphasis for development of solid propellant rocket systems.[1–5] In particular, the Nike-Tomahawk 9 (Refs. 3 and 4) has been flown approximately 75 times to carry 68 kg (150-lb) payloads to approximately 305 km (1,000,000 ft) altitude.

A study[6] was undertaken in 1964 to investigate the possibilities of developing an 0.305-m-diam (12-in.) rocket motor to accommodate larger and heavier payloads. Performance for single-stage applications was to exceed performance of many of the current two-stage systems to enhance reliability. This study ultimately led to the development of the 0.33-m-diam (13-in.) Sandhawk rocket motor (TE-M-473) for Sandia Laboratories by the Thiokol Chemical Corporation. The typical configurations shown in Fig. 1 are either single- or two-stage unguided, solid-propellant, fin-stabilized rockets. The booster for the two-stage systems is drag separated, and either a mechanical or an electrical timer is used to ignite the second stage at a time that maximizes apogee altitude. This paper presents the performance, aerodynamic data, estimated payload-impact dispersion, and flight characteristics of the Sandhawk family of rocket systems.

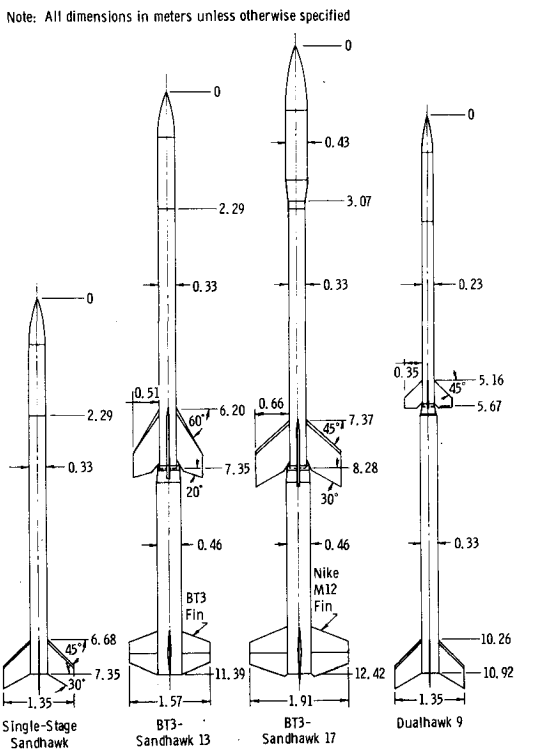

Fig. 1 Sandhawk family of rocket systems.

Presented as Paper 70–1398 at the AIAA 2nd Sounding Rocket Technology Conference, Williamsburg, Va., December 7–9, 1970; submitted December 30, 1970; revision received March 1, 1971. This work was supported by the U.S. Atomic Energy Commission.

* Member of the Technical Staff, Aerothermodynamics Projects Department. Associate Member AIAA.
† Member of the Technical Staff, Aerothermodynamics Projects Department. Member AIAA.

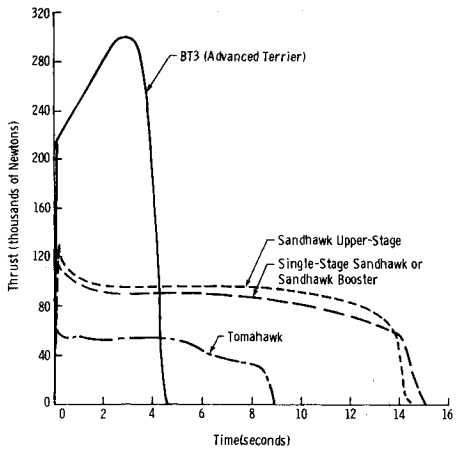

Fig. 2 Sea level thrust-time histories.

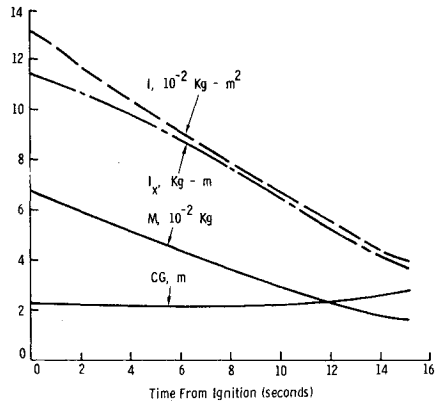

Fig. 3 Estimated Sandhawk (TE-M-473) Rocket Motor mass properties.

Single-Stage Sandhawk[7]

The Sandhawk motor's sea level thrust-time characteristics at 70°F, presented in Fig. 2, were determined from an average of one static firing by Thiokol, one static firing by Sandia, and data reduction of flight test 281-4 launched from Kauai, Hawaii, on May 11, 1967. Motor nominal physical characteristics and weight variation with time given in Fig. 3 were furnished by Thiokol and modified by Sandia to account for differences in total burn time. Other pertinent rocket motor parameters are given in Table 1.

This rocket incorporates either a 0.305- or 0.330-m-diam (12- or 13-in.) ogive cylinder payload which varies from 2.286 to 2.718 m (90–107 in.) in length, and has sufficient volume to carry a wide variety of rocket-launched experiments. Two sets of cruciform fins, those shown with the single-stage, and those shown on the upper stage of the BT3-Sandhawk 13, can be utilized with either diameter payload to allow various flight configurations for a variety of systems hardware.

Data from three flights of this system,[7] two vehicles launched from Tonopah Test Range, Nevada, and one launched from Kauai, Hawaii, indicate that both endo- and exo-atmospheric dynamics of the system are well behaved. Flights 281-3 and 281-4 had exo-atmospheric coning of ±2°, while 281-9 experienced coning of ±10°. The latter's coning angle is attributed to premature payload separation at approximately 76.2 km (250,000 ft) ascending altitude. Performance of flight 281-4, which was stabilized with the fin assembly shown on the upper stage of the BT-3-Sandhawk 13, is shown in Fig. 4.

Advanced Terrier (BT3)-Sandhawk 13 (Ref. 8)

This system's booster is the Advanced Terrier BT3 developed by the Hercules Powder Company. The first-stage booster is stabilized with the standard BT3 fin. Data obtained during flights 281-7 and 281-8 were used to determine the BT3 thrust-time curve presented in Fig. 2. These flights were launched from Johnston Atoll during September and October 1967. The thrust-time characteristics for the Sandhawk, when utilized as the second stage of the BT3-Sandhawk 13 system, are shown in Fig. 2. The motor characteristics are summarized in Table 1. These data were also reduced from flights 281-7 and 281-8, and show a marked departure from the thrust-time characteristics of the single-stage Sandhawk. Five typical configurations, with payloads varying from 2.286 to 3.048 m (90–120 in.) in length, have been extensively evaluated,[8] and no adverse flight characteristics were encountered. The expected general performance for sea level launches of this system is shown in Fig. 4.

Data from nine flights of this system (four vehicles launched from Johnston Atoll and five launched from Kauai, Hawaii) indicate that both the endo- and exo-atmospheric dynamics of this system are well behaved. Exo-atmospheric coning of the following magnitures were observed: 281-7, ±2°; −8, ±3°; −10, ±4°; −11, ±1°; −13, ±7.5°; −14, ±0.5°; −15, ±0.5°; −16, ±2°; and −17, ±0.5°. These data, along with the single-stage flight test data, indicate that misalignment tolerances at Sandhawk motor burnout are extremely small.

The excessive exo-atmospheric coning during flight 281-13 can be directly attributed to erratic roll behavior during

Table 1 Rocket motor parameters, general system performance and fin geometry

Rocket system	Burn time, sec	Total impulse,[a] nt-sec, (lb-sec)	Specific impulse,[a] nt-sec/kg, (lb-sec/lb)	Nozzle exit area, m², (ft²)	Propellant mass, kg, (lb)	Motor diameter, m, (in.)	Pl mass, kg, (lb)	Apogee altitude,[e] km, (ft)	*QE*, deg	Fin planform area, m², (in.²)
Single-stage	15.1	1,200,448 (269,885)	2333.8 (238.0)	0.0774 (0.8330)	514.4 (1134.0)	0.330 (13.0)	90.7 (200)	170 (568,000)	85	0.2813 (436)
BT3-13 and 17	4.6[b]	1,065,882 (239,618)	1916.5 (195.4)	0.1655 (1.7814)	556.1 (1226.0)	0.457 (18.0)	90.7 (200)	426 (1,399,000)	86	0.4020[c] (623)
	14.6[c]	1,215,705 (273,315)		0.0774 (0.8330)	514.4 (1134.0)	0.330 (13.0)	204.5[f] (450)	247[f] (810,000)	86[f]	0.4749[c] (736)
Dualhawk 9	8.9[d]	415,888 (93,500)	2369.1 (242.0)	0.0375 (0.4035)	175.5 (387.0)	0.230 (9.0)	79.4 (175)	543 (1,781,000)	85	0.1335 (207)

[a] Sea level.
[b] First-stage.
[c] Second-stage.
[d] Use single-stage motor parameters for first-stage.
[e] Sea level launch.
[f] BT3-17.

second-stage burn. The Sandhawk fin assemblies for this flight and 281-17 were not dynamically balanced as had been done for previous flights. Both flights showed the roll rate tried to lock in to the natural pitch frequency[9] as the vehicle spun up during second-stage burn. This condition occurred a few seconds later in the trajectory for 281-13, and as a consequence provided a larger initial nutation arm which continued to grow during exit from the atmosphere. All Sandhawk fin assemblies as well as payloads are now dynamically balanced to prevent recurrence of this type of roll behavior.

Advanced Terrier (BT3)-Sandhawk 17

This system is the most recent addition to the Sandhawk family of rocket systems. A bulbous nose, 0.432 m diam (17 in.) is utilized with the Sandhawk motor, along with a larger second-stage fin. The Nike M-12 fin, slightly reduced in span, has been modified to adapt to the Terrier booster to provide adequate stability at launch. Although analytical investigations and wind tunnel tests have been conducted, no firm date has been established for the first ballistic flight.

This system has the ability to accommodate bulky experiments that would present fabrication problems for smaller diameter payloads. The expected performance of this system is summarized in Fig. 4.

Dualhawk 9

The Dualhawk 9 utilizes a Sandhawk motor as a first-stage booster, and a booster fin that is identical to that shown on the single-stage vehicle in Fig. 1. A Tomahawk[3] (TE-M-416) is utilized as an upper-stage motor. The thrust-time characteristics for the single-stage Sandhawk are used for the first stage. The Tomahawk thrust curve shown in Fig. 2 has been reduced from flight test data.

The first flight of this system, 152-128, launched from Kauai, Hawaii, in May 1969, attained an apogee altitude of 528 km (1,733,000 ft) when launched from sea level at an effective elevation angle of 82.5°. This flight exhibited an exo-atmospheric precession arm of 2° relative to the gyro-

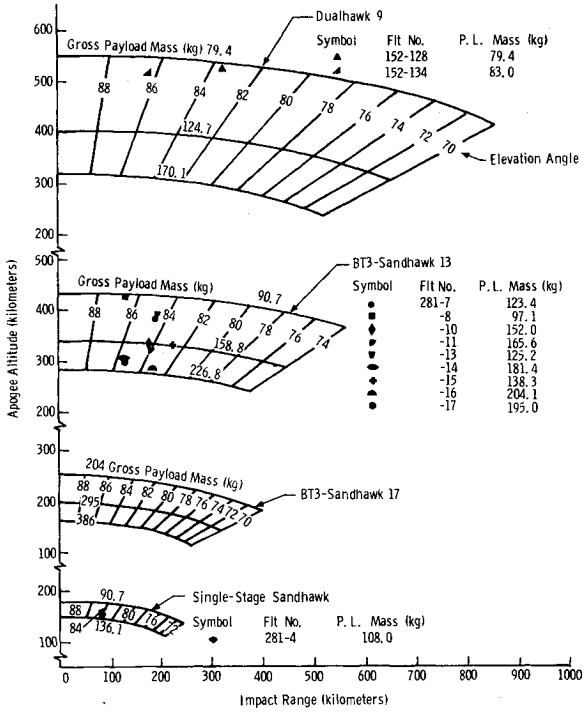

Fig. 4 Sea level performance summary for the Sandhawk family of rocket systems.

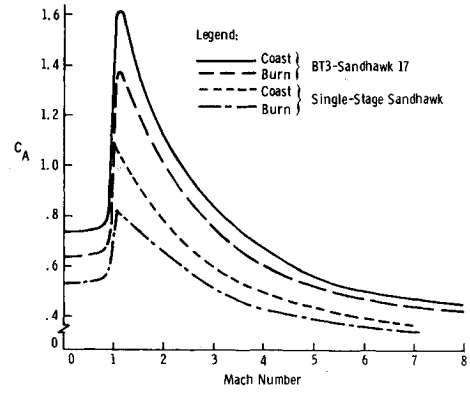

Fig. 5 Axial force coefficient for the single-stage and the BT3-Sandhawk 17 second stage.

uncage position. The second flight, 152-134, was launched from Kauai in October 1970. An apogee altitude of 515.4 km (1,691,000 ft), for a gross payload mass of 83.0 kg (183 lb), was attained for an effective launch elevation angle of 86°. An exo-atmospheric coning motion of ±10° was exhibited during this flight. These payloads were recovered using Sandia Laboratories' Universal Recovery System.[10]

Theoretical performance envelopes as well as the observed performance of the above flights are given in Fig. 4. This figure shows performance for a wide variation of payload masses. These capabilities can be matched with few existing rocket systems.

Aerodynamics

Drag and Static Stability

Stability derivatives were estimated during preliminary system design studies, and the static stability derivatives were confirmed and updated from the results of wind tunnel tests. The coefficients presented here represent the average of both published and unpublished data assimilated from wind tunnel tests.

Single-stage Sandhawk

The static aerodynamic coefficients for the single-stage Sandhawk configurations[7] were determined from wind tunnel tests[11–14] which cover a Mach number range of 0.7 to 11.3. The static stability data used for the configuration shown in Fig. 1 are presented in Figs. 5, 6a, and 6b.

The single-stage Sandhawk axial force coefficient data in Fig. 5 were extensively modified using corrections derived from flight test data of the BT3-Sandhawk 13 second stage. The derivation of these corrections is more fully explained in the section devoted to the BT3-Sandhawk 13 aerodynamic data. The variations of normal force coefficient curve slope and center of pressure with Mach number are presented in Fig. 6. One flight of this configuration with a 0.305-m-diam (12-in.) payload[7] was flown at Tonopah Test Range, Nevada, launch altitude datum of 1.6 km (5350 ft), and the estimated and actual apogee altitude performance agreed within one percent.

BT3-Sandhawk 13

Static aerodynamic coefficients for the BT3-Sandhawk 13 rocket system were determined from wind tunnel tests[11,13,15] which cover a Mach number range of 0.7–11.3. Data from transonic wind tunnel tests of the first stage are given in Fig. 7. Transonic and hypersonic wind-tunnel data for the second

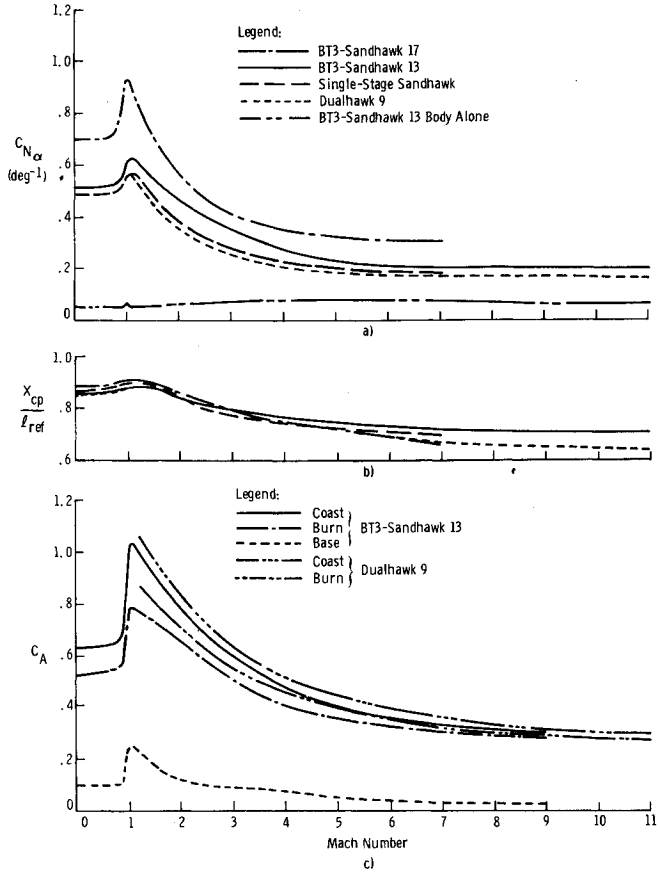

Fig. 6 Static aerodynamic coefficients for single-stage and second-stage vehicles.

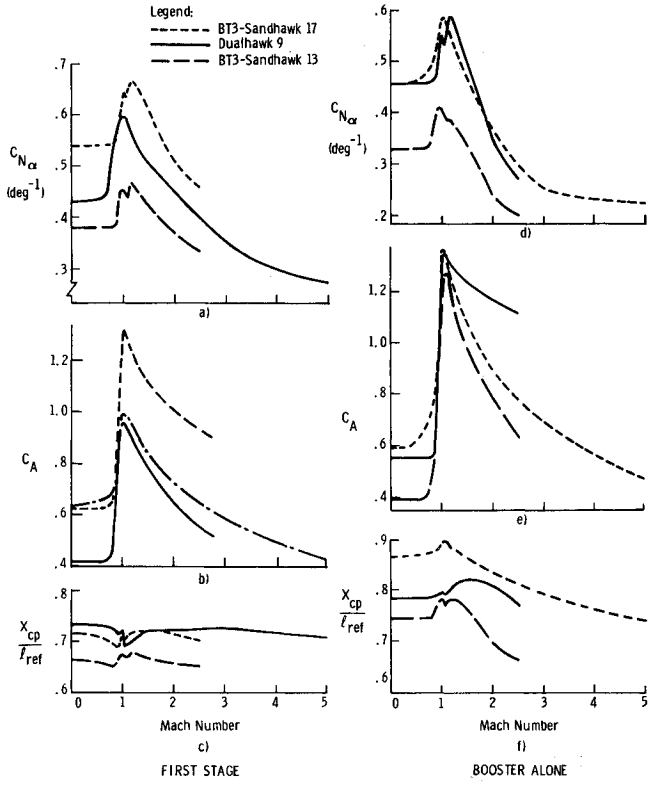

Fig. 7 First-stage and booster-alone aerodynamic data for the BT3-Sandhawk 13 and 17, and the Dualhawk 9.

stage are presented in Fig. 6. The booster alone wind tunnel data in Fig. 7 were determined for a Nike M5E1 booster, but because of booster similarities, these are considered accurate for most analyses applicable to the Advanced Terrier BT3.

The axial force coefficient data for the second stage shown in Fig. 6c are the result of extensively modified wind tunnel data based on flight test data. The solid coasting drag curve was determined from data obtained during flights 281-4, 281-7, and 281-8. Flights 281-7 and 281-8 were BT3-Sandhawk vehicles that provided second-stage coasting drag data for Mach numbers ranges of 1.65 to 2.0 and 8.1 to 8.65. Flight 281-4 was a single-stage flight having the same configuration as the second stage of the BT3-Sandhawk 13; it also provided coasting drag data over a Mach number range of 5.0 to 6.0. Comparing the drag curve established with flight data to wind tunnel data provided a correction to wind tunnel drag data that has been applied to all single-stage[7] and Sandhawk second-stage configurations.[8]

Figure 6c also shows the burning drag curve established by applying the single-stage Sandhawk thrust curve in Fig. 2 to data obtained during the burn phase of 281-4. The difference between the coasting and burning drag curves gives the necessary base drag correction also shown in this figure. This correction is assumed applicable to all single-stage and Sandhawk second-stage configurations. The difference between the coasting drag curve and the uncorrected wind tunnel data is attributed to Reynolds number and model support sting effects.

The first-stage static stability derivatives are based on a reference area of 0.1642 m^2 (1.7671 ft^2) and a reference length of 11.392 m (448.5 in.). The second-stage stability derivatives are based on a reference area of 0.0856 m^2 (0.9217 ft^2), and a reference length of 7.351 m (289.4 in.).

BT3-Sandhawk 17

Static aerodynamic coefficients for the BT3-Sandhawk 17 rocket system were determined from unpublished wind tunnel test data for a Mach number range of 0.7–2.46. Hypersonic aerodynamic characteristics were established from unpublished wind-tunnel test data at Mach numbers of 4.96 and 7.2. The first-stage aerodynamic coefficients are presented in Figs. 7a–c, while the second-stage aerodynamic coefficients are shown in Figs. 5 and 6. The booster alone static aerodynamic coefficients are given in Figs. 7d–f. The drag corrections discussed previously were used to establish the drag curves shown in Fig. 5.

A reference area of 0.1642 m^2 (1.7671 ft^2) and a reference length of 12.421 m (489 in.) are used for the first stage while the second-stage aerodynamic coefficients are based on a reference area of 0.0856 m^2 (0.9217 ft^2) and a reference length of 8.280 m (326 in.).

Dualhawk 9

Static aerodynamic stability derivatives for the Dualhawk 9 rocket system[16] are presented in Figs. 7a–c for the first stage; 6a–c for the second stage; and 7d–f for the Sandhawk booster alone. Mach number ranges of 0.5–3.5 for the first stage and booster alone and 0.7–11.3 for the second stage were used during wind-tunnel tests to obtain the static aerodynamic coefficients.

The first-stage aerodynamic data are based on a reference area of 0.0856 m^2 (0.9217 ft^2) and a reference length of 10.917 m (429.8 in.), while the second-stage data are based on a reference area of 0.041 m^2 (0.4418 ft^2) and a reference length of 5.674 m (233.4 in.)

Dynamic Stability and Roll-Moment Coefficients

The pitching moment and normal force dynamic damping derivatives for slender bodies of general cross section given by Sacks[17] and compared experimentally by Millard and Curry[18]

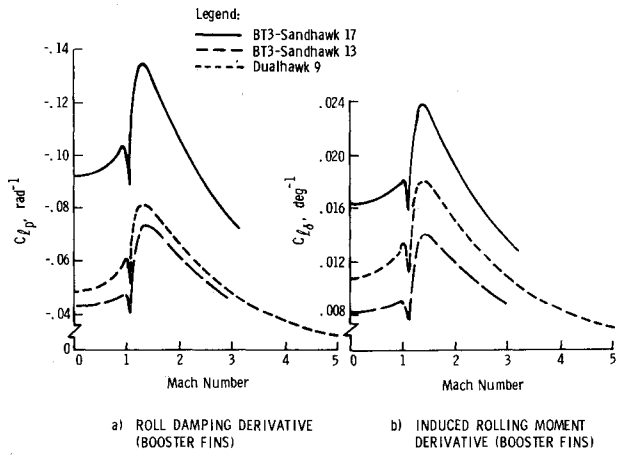

Fig. 8 First-stage induced rolling moment and roll damping coefficients for the BT3-Sandhawk 13 and 17, and the Dualhawk 9.

are

$$C_{m_q} + C_{m_{\dot{\alpha}}} = -2C_{N_\alpha}[(l - X_{c.g.})/l]^2 \quad (1)$$

$$C_{N_q} = 2C_{N_\alpha}[(l - X_{c.g.})/l] \quad (2)$$

and

$$C_{N_{\dot{\alpha}}} = 2\{C_{m_\alpha} + C_{N_\alpha}[(l - X_{c.g.})/l]\} \quad (3)$$

These derivatives, being functions of the normal force coefficient slope and center of gravity, are not represented graphically because of their simplicity. However, these functions are used for trajectory simulation purposes.

The subsonic roll-damping derivative given by Polhamus[19] and modified to include compressibility effects is given by

$$C_{l_p} = -(0.402\pi AR)/\{2\cos\Lambda[((AR^2\beta^2)/(4\cos^4\Lambda)) + 4.0]^{1/2} + 4.0\} \quad (4)$$

The supersonic roll damping derivative established by Bolz and Nicolaides[20] is given by

$$(\beta \cdot C_{l_p})/4 = -\tfrac{1}{3}(1 - \xi^3) + [1/(24\beta^3AR^3)](6\beta AR + 1)(2\beta AR - 1) \quad (5)$$

The relationship between the roll-damping derivative and the induced rolling moment established by Stone[21] is given by

$$C_{l_\delta} = -(64/12\pi)(1 - \xi^2)^{3/2}\, C_{l_p} \quad (6)$$

Eqs. (4–6) are represented graphically for first and second stages in Figs. 8 and 9. Typical roll rate time history profiles are presented in Figs. 10 and 11.

Table 2 Parameters (3σ values) used to evaluate payload impact dispersion

Parameter	BT3-17 and BT3-13 parameters	Dualhawk 9 and single-stage parameters
First stage		
Thrust misalignment		
Angular, deg	0.1	0.1
Offset, m	0.0046	0.0025
Fin misalignment, deg	0.2	0.2
Drag, %	10	10
Inert weight, %	2	2
Motor total impulse, %	3	3
Second stage		
Ignition time, sec	1.5	1.5
Thrust misalignment		
Angular, deg	0.1	0.1
Offset, m	0.0025	0.0030
Fin misalignment, deg	0.2	0.2
Drag, %	10	10
Inert weight, %	2	2
Motor total impulse, %	3	3
Ballistic wind, knots	5	5
Elevation angle (tip off), deg	0.5	0.5
Azimuth setting, deg	0.5	0.5

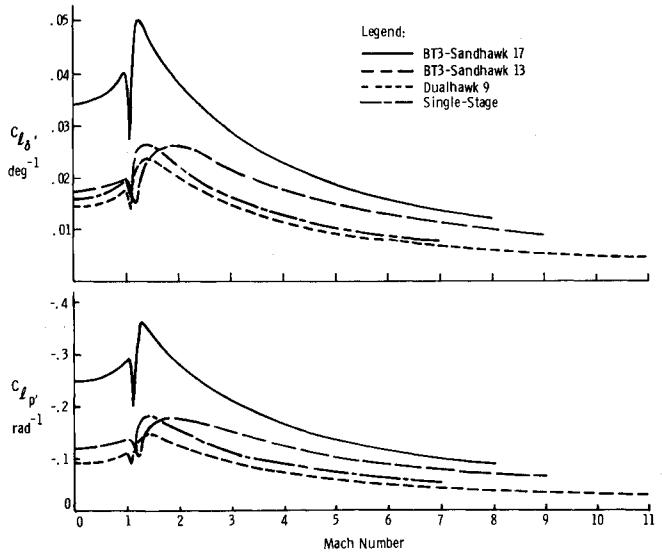

Fig. 9 Induced rolling moment and roll damping coefficients for single-stage and second-stage vehicles.

Vehicle Design Criteria

The design criterion, used by Sandia Laboratories to help ensure suitable sounding rocket flight dynamics during both endo- and exo-atmospheric flight, is to maintain at least a 10% static margin during any portion of atmospheric flight. Since the static margin is implicit in the computation of the vehicle static restoring moment, this criterion, coupled with Eq. (1), tends to assure that any adverse motion attributed to system tolerances during motor burn will be damped. Typical rigid-body static margin-time history profiles are shown graphically in Figs. 10 and 11.

A second criterion, used to enhance exo-atmospheric vehicle dynamics and to help minimize impact dispersion, is to maintain the correct relationship between the rigid-body

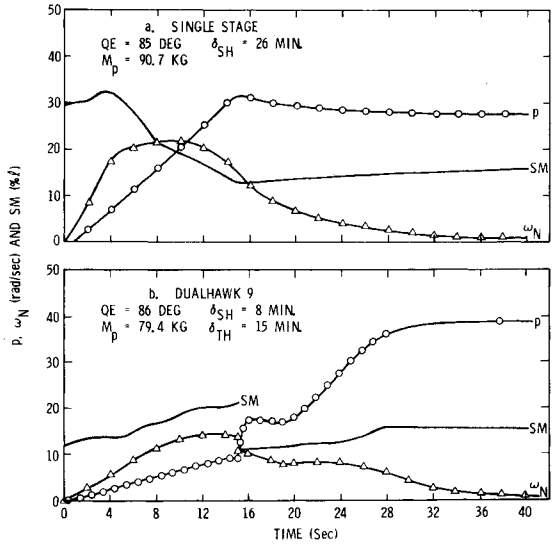

Fig. 10 Single-stage Sandhawk and Dualhawk 9 roll rate, natural pitch frequency, and static margin variations with time.

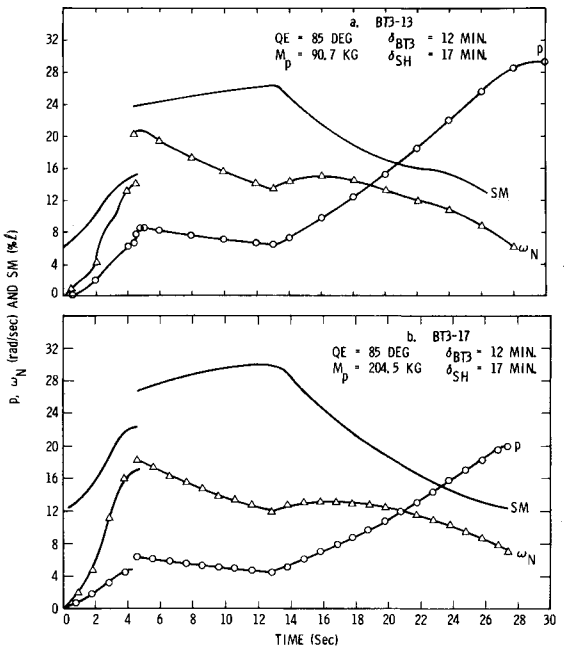

Fig. 11 BT3-Sandhawk 13 and 17 roll rate, natural pitch frequency, and static margin variations with time.

undamped natural pitch frequency and the induced roll rate. The correct induced roll rate gyroscopically stabilizes the system exo-atmospherically and helps to prevent roll lock-in. Typical undamped natural pitch frequency time history profiles related to the induced roll rate are also represented in Figs. 10 and 11.

Evidence that the correct induced roll rate and undamped natural pitch frequency relationship has been maintained is obtained from flight test data with the exception of the BT3 Sandhawk 13 flights discussed previously. The stable platform[22] pitch and yaw data for all flights show very little amplification when the roll rate approaches and crosses the undamped natural pitch frequency.

Performance

Theoretical system performance for all vehicles was predicted using the Air Force six-degree-of-freedom generalized computer program.[23] The results of theoretical trajectories presented in this paper, together with dispersion estimates and the evaluation of wind effects for payload and booster impact predictions,[7,8] are based on this computer program.

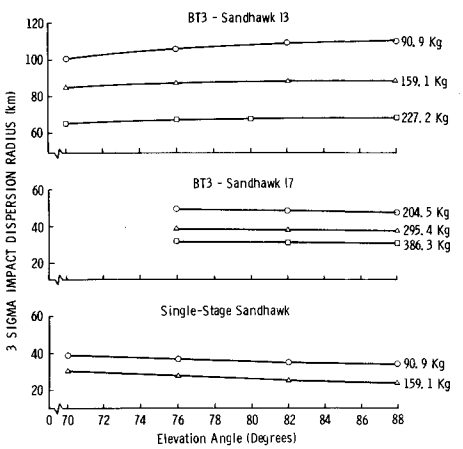

Fig. 12 Predicted 3σ impact dispersion radii for the Sandhawk family of rocket systems.

The apogee altitude variation with impact range data for all configurations given in Fig. 4 were fitted with Schaechter's[24] empirical performance equations and found to represent the trajectory simulations adequately for gross payload weights of interest. The use of Schaechter's equations permits a minimum number of trajectory simulations for the estimated system performance.

The expected dispersion for this family of rocket systems has been determined using the Air Force trajectory program.[23] A normal circular distribution[25] is used to determine the dispersion of an impacting vehicle about the nominal impact point; i.e., a 1σ radius represents 39.35% of the rocket impact points; 2σ and 3σ represent 86.47% and 98.89%, respectively. Table 2 presents the estimated magnitudes of the variables that are considered as contributors to the 3σ dispersion radii for this family of rocket systems. (The values for the single-stage Sandhawk are obtained from column 2 by neglecting the second stage.)

Figure 12 shows the estimated values of the 3σ dispersion radius at payload impact for all systems except the Dualhawk 9. For the Dualhawk 9, with $QE = 86°$, a payload mass of 79.4 kg (175 lb), and an assumed launcher rail length of 4.88 m (16 ft), the 3σ radius is 164.6 km.

Larger payload weights increase the static margin, and hence, reduce the effects of thrust misalignments while increasing the wind effectiveness. The analyses conducted to obtain the data in Fig. 12 assume that the systems have a minimum rail guidance of 3.05 m for the single-stage Sandhawk; 3.81 m for the BT3-Sandhawk 13; and 5.03 m for the BT3-Sandhawk 17. It is worth noting that the low-roll rate and/or small static margin during booster burn yield large values of the 3σ dispersion radius. Dispersion at booster and unfired second-stage impacts have been determined for all systems,[7,8,17] except for the BT3-Sandhawk 17.

Three flights of the single-stage Sandhawk have all impacted within the predicted 1σ value of the dispersion radius. Two flights of the Dualhawk 9 and nine flights of the BT3-Sandhawk 13 have all impacted within the predicted 3σ values.

Conclusions

The rocket systems comprising the Sandhawk family are versatile research vehicles. These systems have shown good reliability and performance for 79.4 — 385.6 kg payloads. Their payloads are voluminous (0.07—0.36 m^3 have been analyzed) and can be adapted to a variety of scientific experiments. These vehicles have exhibited good dynamic characteristics during both endo- and exo-atmospheric flight.

References

[1] Matejka, D. Q., "Aeroballistics of the Nitehawk 12 Rocket System," SC-DR-68-585, Oct. 1968, Sandia Labs., Albuquerque, N. Mex.

[2] Wilson, G. G., Stone, G. W., and Barton, W. R., "Flight Test Data Obtained During the Development of the Strypi II and Strypi IV Rocket Systems for the Test Readiness Program," SC-RR-65-282, (OUO), Jan. 1967, Sandia Labs., Albuquerque, N. Mex.

[3] Connell, G. M. and Stone, G. W., "Performance Summary for the Sandia Nitehawk 9 Rocket System," SC-RR-65-561, July 1966, Sandia Labs., Albuquerque, N. Mex.

[4] Stone, G. W., "Summary and Analysis of Flight Data on the Sandia Nitehawk 9 Rocket System," SC-DR-66-664, March 1967, Sandia Labs., Albuquerque, N. Mex.

[5] Gardner, R. E., "Aeroballistic Development of the Single-Stage Tomahawk Sounding Rocket System," SC-RR-66-2608, May 1967, Sandia Labs., Albuquerque, N. Mex.

[6] Wilson, G. G., "Development Criteria for a 12-Inch Diameter Rocket Motor to be Used in an Instrumentation Rocket System," SC-TM-65-216 (OUO), Aug. 1965, Sandia Labs., Albuquerque, N. Mex.

[7] Wilson, G. G. and Stone, G. W., "Aeroballistic, Performance, Wind Effects and Payload Impact Dispersion Analyses and Flight Test Data for the Single-Stage Sandhawk Rocket System," SC-DR-69-291, July 1969, Sandia Labs., Albuquerque, N. Mex.

[8] Wilson, G. G., "Aeroballistic, Performance, Wind Effects, and Payload Impact Dispersion Analyses and Flight Test Data for the Two-Stage Terrier (BT-3)—Sandhawk Rocket System," SC-DR-69-304, July 1969, Sandia Labs., Albuquerque, N. Mex.

[9] Price, D. A., Jr., "Sources, Mechanisms, and Control of Roll Resonance Phenomena for Sounding Rockets," *AIAA Sounding Rocket Vehicle Technology Specialist Conference*, AIAA, New York, 1967.

[10] Johnson, D. W., "Development of Recovery Systems for High Altitude Sounding Rockets," *Journal of Spacecraft and Rockets*, Vol. 6, No. 4, April 1969, pp. 489–491.

[11] Hunter, J. A., "Three-Component Wind Tunnel Force Test of Three Finned and One Finless Sandhawk Configurations at Mach 4.9, 7.3, and 11.3," SC-TM-66-2615, Jan. 1967, Sandia Labs., Albuquerque, N. Mex.

[12] Tate, R. E., "Three-Component Static Force Test of a Sandhawk Model with New Fins at Mach Numbers of 4.91 and 7.28," SC-TM-67-3028, Jan. 1968, Sandia Labs., Albuquerque, N. Mex.

[13] Millard, W. A., "Results of Wind-Tunnel Force Tests of the Sandhawk, Nike-Sandhawk, and Advanced Terrier Sandhawk at Several Mach Numbers Between 0.7 and 3.0," SC-DR-68-101, April 1968, Sandia Labs., Albuquerque, N. Mex.

[14] Tate, R. E., "Three-Component Static Force Test of a Sandhawk Model with New Fins at Mach Numbers of 0.69 through 3.0," SCTM-68-746, Nov. 1968, Sandia Labs., Albuquerque, N. Mex.

[15] Tate, R. E., "Three-Component Force Test of a Nike Booster at Mach Numbers from 0.70 through 2.46," SC-TM-68-553, Sept. 1968, Sandia Labs., Albuquerque, N. Mex.

[16] Wilson, G. G., "Range Safety for the Dualhawk 9 Rocket System," Feb. 1969, Pacific Missile Range.

[17] Sacks, A. H., "Aerodynamic Forces, Moments, and Stability Derivatives for Slender Bodies of General Cross Section," TN-3283, Nov. 1954, NACA.

[18] Millard, W. A. and Curry, W. H., "A Thin Strap Support for the Measurement of the Dynamic Stability Characteristics of High Fineness Ratio Wind Tunnel Models," *Journal of Spacecraft and Rockets*, Vol. 7, No. 7, July 1970, pp. 854–858.

[19] Polhamus, E. C., "A Simple Method of Estimating the Subsonic Lift and Damping in Roll of Sweptback Wings," TN-1862, April 1949, NACA.

[20] Bolz, R. E. and Nicolaides, J. D., "A Method of Determining Aerodynamic Coefficient from Supersonic Free-Flight Tests of a Rolling Missile," *Journal of the Aeronautical Sciences*, Vol. 17, No. 10, Oct. 1950, pp. 609–621.

[21] Stone, G. W., "The Transient Rolling Motion of a Finned Slender Body," SC-TM-210-62(71), Sept. 1962, Sandia Labs., Albuquerque, N. Mex.

[22] Sinnot, N. F. and Rasmussen, R. O., "Performance and Application of a Miniature Roll-Stabilized Gyro Platform," SC-R-65-1023, Oct. 1965, Sandia Labs., Albuquerque, N. Mex.

[23] "Six-Degree-of-Freedom Flight-Path Study Generalized Computer Program," FDL-TDR-64-1, Pts. 1 and 2, Vol. I, Oct. 1964, Air Force Flight Dynamics Lab.

[24] Schaechter, W., "Sounding Rocket Performance Approximations," Presented at Unguided Rocket Ballistics Meteorology Conference, New Mexico State Univ., Las Cruces, N. Mex., Oct. 31–Nov. 2, 1967.

[25] Korn, G. A. and Korn, T. M., "Probability Theory and Random Processes," *Mathematical Handbook for Scientists and Engineers*, McGraw-Hill, New York, 1968, pp. 585–663.